nature neuroscience

Role of rodent secondary motor cortex in value-based action selection

Jung Hoon Sul[1], Suhyun Jo[1,2], Daeyeol Lee[3] & Min Whan Jung[1,2]

Despite widespread neural activity related to reward values, signals related to upcoming choice have not been clearly identified in the rodent brain. Here we examined neuronal activity in the lateral (AGl) and medial (AGm) agranular cortex, corresponding to the primary and secondary motor cortex, respectively, in rats performing a dynamic foraging task. Choice signals, before behavioral manifestation of the rat's choice, arose in the AGm earlier than in any other areas of the rat brain previously studied under free-choice conditions. The AGm also conveyed neural signals for decision value and chosen value. By contrast, upcoming choice signals arose later, and value signals were weaker, in the AGl. We also found that AGm lesions made the rats' choices less dependent on dynamically updated values. These results suggest that rodent secondary motor cortex might be uniquely involved in both representing and reading out value signals for flexible action selection.

Value-based decision making consists of two broad steps of valuation and selection. Previous studies have shown value-related neuronal activity in a number of different brain structures such as the striatum[1–3], parietal cortex[4–6], anterior cingulate cortex (ACC)[7,8], orbitofrontal cortex (OFC)[8–10] and other parts of the prefrontal cortex (PFC)[8,11] in rats and monkeys. Also, after the outcome of the animal's choice is revealed, neuronal activity that is related to reward prediction error (RPE), namely the difference between the actual and predicted rewards, is found in multiple brain areas including midbrain dopamine regions[12], OFC[8] and the striatum[2]. These results indicate that the valuation of action outcomes engages multiple brain structures.

The neural system responsible for making a choice (selecting a single action from multiple alternatives) based on values of expected outcomes has been more elusive. Although previous studies have found future choice-related neural signals in several brain areas such as the striatum[1], dorsolateral PFC[13], supplementary eye field (SEF)[14] and parietal cortex[6,15,16] in monkeys during a free-choice task, choice-related signals in multiple brain structures do not necessarily indicate that they are all involved in the final action selection process. Whereas valuation can be processed in parallel, choice must involve a process that selects a single action from multiple alternatives that is to be executed by the motor system. Thus, although several brain regions might display upcoming choice signals in a given behavioral setting, it is likely that action selection takes place in a specific neural system and that the resulting choice signals then propagate to other systems for the purpose of executing or evaluating the chosen action. Therefore, to identify the neural system responsible for final action selection, it would be important to compare relative time courses of choice signals across different brain regions and to examine the effects of local lesion or inactivation on the choice behavior of animals under the same behavioral setting.

Another important question is how different components of value-based decision making, namely value representation, action selection and action evaluation, overlap across different brain structures. Given that many brain areas conveying value signals tend to encode upcoming actions chosen by the animal (see above), it is likely that these functions are served by partially overlapping brain structures. However, the exact distribution of these functions remains unclear, partly because only a few studies have examined all of these signals in multiple brain areas under the same experimental setting (for example, refs. 8,11,17).

We investigated these issues in the rat brain. In our previous studies with rats[2,8,18], value-related neural signals have been found in the lateral OFC, medial PFC (dorsal ACC, prelimbic cortex and infralimbic cortex), dorsal striatum and ventral striatum. By contrast, clear signals that were related to upcoming choice were found in none of these brain structures. We therefore hypothesized that upcoming choice signals would be found in a motor structure. The first aim of this study was to test this prediction, and it was supported by the data. The second aim was to test whether upcoming choice signals coexist with value signals at the final stage of decision making. Our results showed that the secondary motor cortex of the rat processes both action selection and value signals. We also found that the lesion in the same area impairs flexible, value-based decision making.

RESULTS

Choice behavior and movement trajectory

Three rats performed a dynamic foraging task[19] (**Fig. 1**), choosing freely between two goals that delivered a fixed amount of water reward with different probabilities. Although reward probabilities were constant within a block of 35–45 trials (four blocks per session), water was delivered stochastically in each trial and no sensory stimuli signaled block transitions, so that the rats could detect changes in reward

[1]Neuroscience Laboratory, Institute for Medical Sciences, Ajou University School of Medicine, Suwon, Korea. [2]Neuroscience Graduate Program, Ajou University School of Medicine, Suwon, Korea. [3]Department of Neurobiology, Yale University School of Medicine, New Haven, Connecticut, USA. Correspondence should be addressed to M.W.J. (min@ajou.ac.kr).

Received 2 March; accepted 6 June; published online 14 August 2011; corrected after print 12 April 2012; doi:10.1038/nn.2881

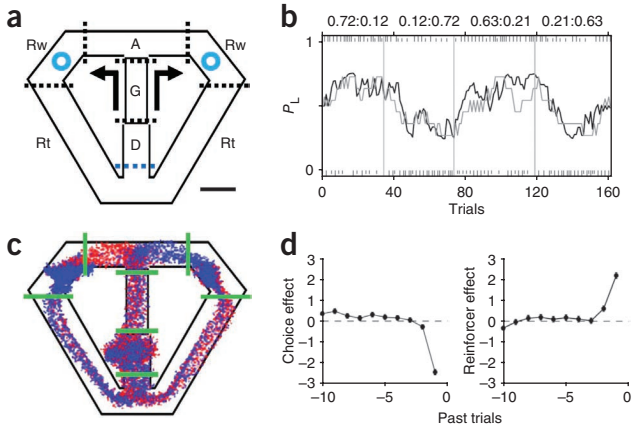

Figure 1 Behavioral task and choice behavior. (**a**) Rats were allowed to choose freely between two locations (blue circles) that delivered water with different probabilities. The task was divided into five stages: delay (D), go (G), approach to reward (A), reward (Rw) and return (Rt) stages. Dotted lines indicate approximate stage transition points (blue dotted line, onset of delay stage, which marks the beginning of a trial). Arrows indicate movement directions. Scale bar represents 10 cm. (**b**) Choice behavior of a rat during an example behavioral session. The gray line shows the probability for the rat to choose the left goal (P_L; moving average of ten trials). The black line indicates the probability of choosing the left goal in the reinforcement learning model. Tick marks denote trial-by-trial choices of the rat (top bar, left choice; bottom bar, right choice; long, rewarded; short, unrewarded) and vertical lines denote block transitions. Reward probabilities for each block are indicated at the top. (**c**) Movement trajectories during an example session. Each dot indicates the rat's head position (sampling frequency, 60 Hz). Green solid lines indicate stage transitions. Beginning from the reward onset, blue and red dots indicate trials associated with the left and right upcoming choice of the rat, respectively. Trials were decimated (3 to 1) to enhance visibility. (**d**) Effects of past choices and their outcomes on the current goal choice for one rat. The ordinate shows the coefficients of a logistic regression model. Positive coefficients indicate an increased likelihood for the rat to repeat rewarded past choices (reinforcer effect) or past goal choices irrespective of their outcomes (choice effect). Error bars represent s.e.m.

probabilities only by trial and error. Nevertheless, the rats quickly detected changes in relative reward probabilities after a block transition and biased their choices toward the goal with a higher reward probability, which was well described by a reinforcement learning model (**Fig. 1b**). The rats obtained rewards in 61.7 ± 4.5% (mean ± s.d.) of trials, which is significantly lower than the amount of rewards expected for the reinforcement learning model with optimal parameters (72.1 ± 2.3%; *t*-test, $P < 0.001$). A logistic regression analysis showed that past rewards from up to two previous trials biased the rats to repeat the same goal choice, with the reward from the most recent trial having the greatest effect. There was also a tendency for the rats to alternate their goal choices (**Fig. 1d**).

A trial was divided into delay, go, approach to reward, reward consumption and return stages, as in our previous studies[2,8] (**Fig. 1a**). The rats showed a stereotyped pattern of movements on the maze (**Fig. 1c**). The rat's movement trajectory during the early delay stage reflected the previous goal choice (initial 0.78 ± 0.16 s of the delay stage), but this was not the case during subsequent behavioral stages. The onset of the approach stage was when the rat's movement trajectory began to diverge depending on the animal's upcoming goal choice (that is, the first behavioral manifestation of the rat's goal choice; **Supplementary Fig. 1**). The analysis of the rat's movement trajectory revealed, as in our previous study[2], that the movement trajectory did not vary with the rat's future goal choice in any of the behavioral stages before the onset of the approach stage.

Neural signals for choice

Single units were recorded simultaneously from rostral parts of the AGl and AGm (**Fig. 2**) in the right hemisphere of the three rats. A total of 227 and 411 well-isolated single units (≥500 spikes during each recording session) were recorded from the AGl and AGm, respectively. We first analyzed neural activity related to the rat's choice, its outcome and their interaction in the current and two preceding trials using a multiple regression analysis. **Figure 3a** shows the fractions of neurons that significantly (see equation (1), Online Methods) modulated their activity according to these behavioral variables in non-overlapping 500-ms time windows across different behavioral stages ($P < 0.05$). Neural signals for the rat's upcoming choice in the current trial ($C(t)$) were low during the delay stage but began to increase during the go stage first in the AGm and then in the AGl (**Fig. 3a**). By analyzing neural activity with a higher temporal resolution, we found that the onset of the upcoming choice signal (see Online Methods for its definition) was approximately 500 and 150 ms before the onset of the approach stage in the AGm and AGl, respectively, and that the fraction of choice-encoding neurons was significantly larger in the AGm both before and after the onset of the approach stage (χ^2-test, $P < 0.05$; **Fig. 3b**). A similar pattern was observed when the time course of the upcoming choice signal was examined by decoding the rat's goal choice from population activity (**Fig. 3c**). The distribution of the choice signal onset for individual neurons was also different between the AGm and AGl (**Fig. 3d,e**). Among a total of 95 AGm neurons showing significant choice-related activity during the 500-ms time period before the approach stage onset, 48 (50.5%) and 47 (49.5%) discharged at higher rates in the left and right goal-choice trials, respectively, values that are not significantly different from each other (χ^2-test, $P = 0.918$). The corresponding numbers of AGl neurons were 16 (55.2%) and 13 (44.8%), respectively, also not significantly different from each other ($P = 0.732$).

Large fractions of neurons encoded signals for the rat's chosen action ($C(t)$) after the rat revealed its choice (approach, reward and return stages; **Fig. 3a**). It should be noted that sensory and motor events associated with left and right goal choices were different during these subsequent behavioral stages. Neural signals for already chosen actions might reflect the rat's choice or sensorimotor features (such as movement direction) that were different for the left and right sides of the maze. Many neurons encoded reward (that is, choice outcome, $R(t)$) or chosen action × reward interaction ($X(t)$) after the outcome of the rat's choice was revealed (reward stage; **Fig. 3a**). These signals, especially chosen action signals, persisted until the next trial so that low but significant previous choice ($C(t-1)$), previous

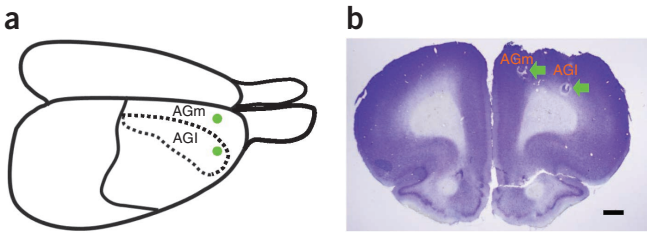

Figure 2 Recording sites. Single units were recorded from the rostral AGm and AGl. (**a**) Dorsolateral view of the rat brain. Green dots indicate approximate electrode implantation sites. (**b**) Coronal section of the brain stained with cresyl violet. Green arrows indicate marking lesions. Scale bar represents 1 mm.

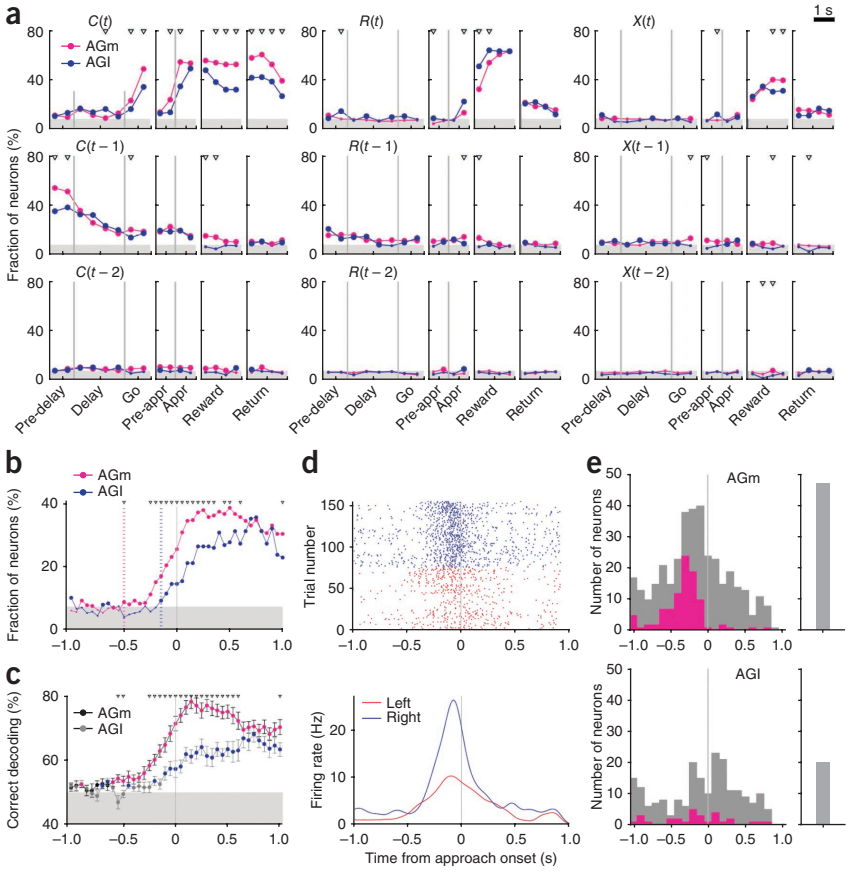

Figure 3 Neural signals for the rat's choice and reward. (**a**) Fractions of neurons that significantly modulated their activity according to the rat's choice (*C*), reward (*R*), or their interaction (*X*) in the current (*t*) and previous (*t* – 1 and *t* – 2) trials in non-overlapping 500-ms time windows (see equation (1), Online Methods). Pre-delay stage, last 1 s of the return stage; pre-approach stage (Pre-appr), last 1 s of the go stage; Appr, approach stage. The vertical lines indicate the onset of a behavioral stage. Large dots indicate that the fraction is above chance level (binomial test, $P < 0.05$), and triangles indicate significant differences between AGl and AGm (χ^2-test, $P < 0.05$). The gray shading indicates the mean of the minimum fractions significantly above chance, which is slightly different for the AGm and AGl. (**b**) Fractions of current choice (*C*(*t*))-encoding neurons plotted in a 100-ms time window, advanced in 50-ms time steps. The magenta and blue dotted lines indicate the onsets of the current choice signals for the AGm and AGl, respectively (see Online Methods). (**c**) Neuronal population decoding of the rat's goal choice (percentage correct decoding) (100-ms window, 50-ms time steps). Magenta (AGm) and blue (AGl) symbols indicate significant differences from the chance level (50%; *t*-test, $P < 0.05$). Triangles indicate significant differences between the two areas (*t*-test, $P < 0.05$). Error bars represent s.e.m. (**d**) An example AGm neuron that modulated its activity according to the rat's upcoming goal choice. Top, spike raster; bottom, spike density functions (Gaussian kernel, $\sigma = 50$ ms). (**e**) Distribution of the choice signal onset for individual neurons (see Online Methods). Magenta indicates neurons that significantly modulated their activity according to the rat's upcoming choice during the 500-ms time window before the approach onset ($P < 0.05$; see equation (1), Online Methods). Gray indicates the remaining neurons. Neurons that were determined not to have a choice onset during 1-s time periods before and after the approach onset are plotted separately on the right.

reward (*R*(*t*–*1*)) and previous interaction (*X*(*t*–*1*)) signals were observed ($P < 0.05$; **Fig. 3a**). Similar results were obtained when the analysis was based on the magnitudes of regression coefficients rather than the fractions of statistically significant neurons (**Supplementary Fig. 2a**). Example neurons that modulated their activity according to the rat's choice or reward in the previous trial are shown in **Supplementary Figure 3**.

Neural signals for decision value

Neural signals related to valuation process were examined by relating neural activity to action values that were estimated with a model-based reinforcement learning algorithm[19] (stacked probability algorithm; **Supplementary Note**). The reinforcement learning algorithm predicted the rat's actual choices well (**Fig. 1b**), suggesting that the rat's subjective values for alternative actions were reliably estimated by this model. We examined neural signals for decision value (Δ*Q*), which was defined as the difference between the left and right action values ($Q_L - Q_R$), and chosen value (Q_c), which was the value of chosen action in a given trial[8] (see equation (2), Online Methods). Decision value and chosen value would be useful in deciding which goal to choose and evaluating the value of chosen action, respectively. Decision value signals fluctuated around the chance level in the AGl. The AGm conveyed significant but still weak decision value signals ($P < 0.05$), so that the difference in the strength of decision value signals was not large between the AGm and AGl (**Fig. 4a**). Given that decision value signals are also weak in the OFC, medial PFC

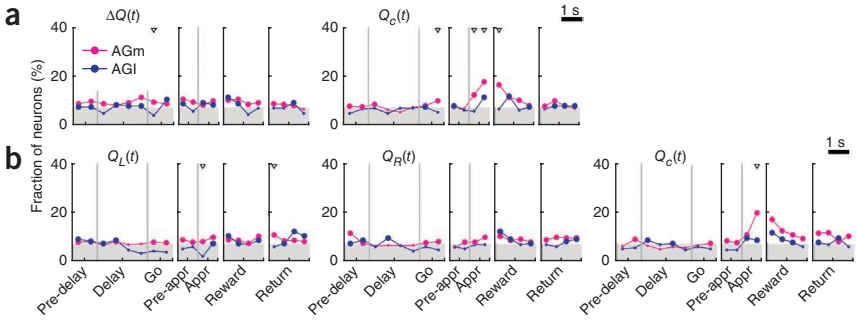

Figure 4 Neural signals for values. (**a**) Fractions of neurons that significantly modulated their activity according to decision value (Δ*Q*) or chosen value (Q_c) in non-overlapping 500-ms time windows (see equation (2), Online Methods). (**b**) Fractions of neurons that significantly modulated their activity according to the left or right action value ($Q_L(t)$ or $Q_R(t)$, respectively). The same regression analysis (see equation (2), Online Methods) was performed with decision value replaced with the left and right action values. Same format as in **Figure 3a**.

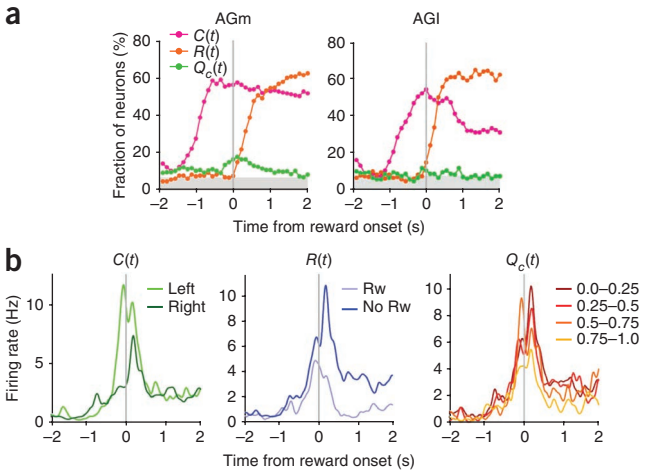

Figure 5 Convergence of neural signals for chosen action, reward and chosen value in the AGm. (**a**) Fractions of neurons that significantly modulated their activity according to chosen action, reward or chosen value shown in a 500-ms time window, advanced in 100-ms time steps around the time of reward stage onset. (**b**) An example AGm neuron that significantly modulated its activity according to chosen action, reward and chosen value in the reward stage ($P < 0.05$). Spike density functions (Gaussian kernel, $\sigma = 50$ ms) are shown separately for different choices (left versus right), different choice outcomes (rewarded versus unrewarded) or different levels of chosen value.

and the striatum in rats[2,8], this finding suggests that decision value signals might be only weakly represented as persistent activity in multiple areas of the rat brain. An example AGm neuron that modulated its activity according to decision value is shown in **Supplementary Figure 3**.

We also examined neural signals for action value by replacing decision value with the left and right action values in the regression (see equation (2), Online Methods). Unlike decision value signals, action value signals were below chance level during the delay stage in the AGm (**Fig. 4b**). There were only 14 AGl neurons out of 227 (6.2%; binomial test, $P = 0.248$) and 24 AGm neurons out of 411 (5.8%; binomial test, $P = 0.246$) that significantly modulated their activity according to the value of at least one action (Q_L or Q_R; $P < 0.025$, $\alpha = 0.05$ was corrected for multiple comparisons) during the last 1 s of the delay stage. The fraction of action value-encoding neurons during the last 1 s of the delay stage (5.8%) was significantly lower than that of decision value-encoding neurons (11.2%; χ^2-test, $P = 0.006$) in the AGm.

Neural signals for chosen value

Chosen value signals arose after the rat revealed its choice (approach stage) and then slowly decayed during the reward stage in the AGm (**Fig. 4**). Chosen value signals in the AGl were weaker than in the AGm. During the 1-s period centered at the onset of the reward stage, 66 AGm neurons (16.1%; binomial test, $P < 0.001$) and 17 AGl neurons (7.5%; binomial test, $P = 0.065$) modulated their activity according to chosen value, and this difference between the two areas was statistically significant (χ^2-test, $P = 0.002$). Similar results were obtained when the analysis was based on the magnitudes of regression coefficients (**Supplementary Fig. 2b**). For some neurons in the AGm and AGl, chosen value signals changed significantly depending on the rat's chosen action: 43 AGm neurons (10.5%) and 24 AGl neurons (10.6%) showed significant chosen action × chosen value interaction (**Supplementary Fig. 4**).

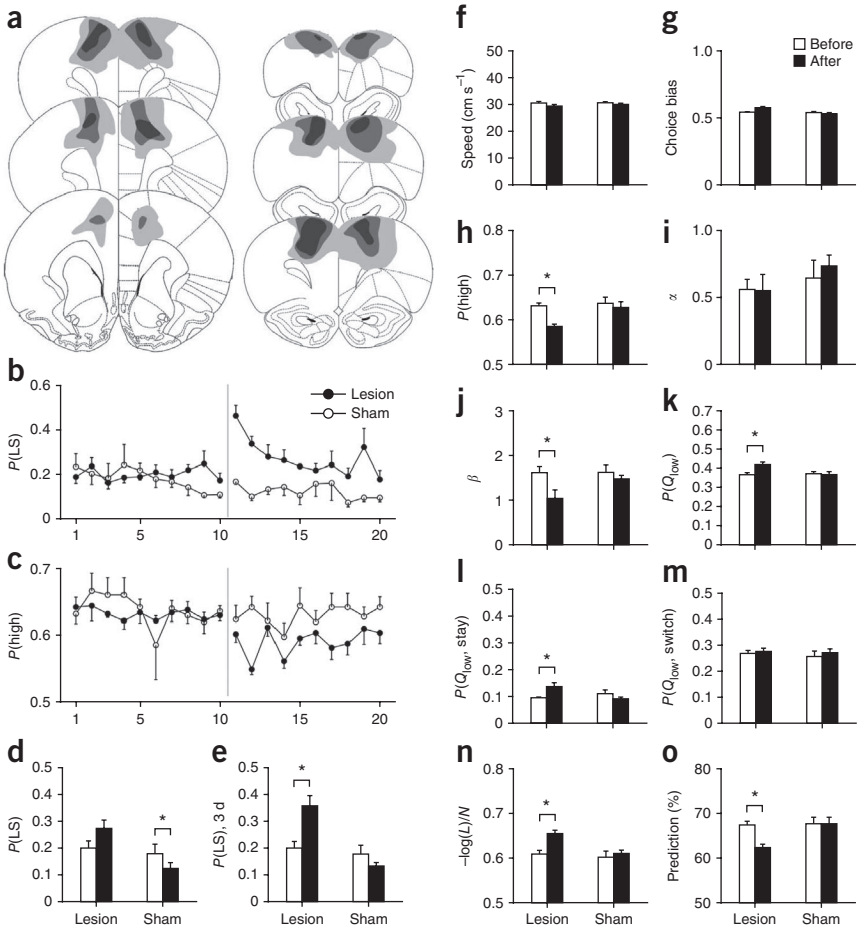

Figure 6 Effects of AGm lesions. (**a**) The extent of AGm lesions. The diagram shows the extent of maximal (light gray), representative (medium gray) and minimal (dark gray) lesions across five rats. Panel **a** is modified with permission from Elsevier (from ref. 46). (**b**,**c**) Time courses for the probabilities of lose-stay (P(LS)) and for selecting the higher reward probability goal in each block (P(high)). (**d**) P(LS) averaged for 10 d before and after lesions. (**e**) P(LS) for the initial 3 d following lesions (P(LS), 3 d) was compared with P(LS) during the pre-lesion period (10 d). (**f**) Mean running speed across go, approach and return stages before and after AGm or sham lesions. (**g**) Choice bias (fraction of the choice for a preferential goal in a given session). (**h**) P(high) before and after lesions. (**i**,**j**) Learning rate (α) and inverse temperature (β) of the reinforcement learning model. (**k**) The probability of choosing the lower action-value goal ($P(Q_{low})$). (**l**,**m**) $P(Q_{low})$, shown separately for staying ($P(Q_{low}$, stay)) and switching ($P(Q_{low}$, switch)) trials. (**n**) Normalized negative log-likelihood ($-\log(L)/N$) of the reinforcement learning model. (**o**) Prediction of the rat's choices by the reinforcement learning model (percentage correct). The data in (**d**–**o**) are averaged values during the pre-lesion and post-lesion periods (10 d each), except for P(LS), 3 d (**e**). Asterisks indicate significant differences (paired t-test, $P < 0.05$). Error bars represent s.e.m.

To examine whether chosen value signals are combined with other signals necessary to evaluate chosen action, we examined neural signals for the rat's chosen action, reward and chosen value around the time of reward stage onset at a higher temporal resolution (100-ms time steps). All three signals were robustly present in the AGm during the early reward stage (**Fig. 5a**). Of 36 AGm neurons out of 411 (8.8%) that concurrently conveyed signals for reward and chosen value during the first 1 s of the reward stage, 26 (72.2%) also conveyed neural signals for the rat's chosen action (**Fig. 5b**). Thus, some AGm neurons conveyed all the signals necessary to compute RPE and update the value of chosen action. It should be noted that the likelihood of a false negative (a type II error) increases when multiple tests are applied in conjunction; the expected number of AGm neurons that encode both reward and chosen value by chance is only 1.0 among 411 neurons. Further analyses suggested that these signals are combined to compute RPE as well as to update the value of chosen action in the AGm (**Supplementary Fig. 5**).

Effects of AGm lesions

Coding of both choice and value signals in the AGm suggests that this area might be critical for value-based action selection. We tested this possibility further by examining the behavioral effects of bilateral lesions of the rostral AGm (**Fig. 6**). AGm lesions induced no significant changes in the rat's running speed (**Fig. 6f**) or choice bias (**Fig. 6g**). However, both short-lasting and long-lasting changes were observed in several related measures of the rat's choice behavior (see **Supplementary Table 1** for the results of statistical analyses). The rat's tendency to repeat the same goal choice after failing to obtain a reward (lose–stay) increased transiently during the 3 to 5 d after lesioning (**Fig. 6b**,**d**,**e**). By contrast, a decrease in the probability of choosing the goal with higher reward probability persisted for 10 d (**Fig. 6c**,**h**).

Long-lasting changes were also observed in several reinforcement learning model-related measures. The inverse temperature (β) of the reinforcement learning model decreased after lesions, whereas there was no significant change in the learning rate (α; **Fig. 6i**,**j**). In addition, the lesioned rats were more likely to choose the goal that was associated with a lower action value than the alternative (**Fig. 6k**). In particular, they were more likely to repeat the goal choice that was associated with a lower action value (**Fig. 6l**), whereas the likelihood of switching their choices to a lower value goal was unaffected (**Fig. 6m**). Finally, the goodness of fit for the reinforcement learning model (log-likelihood normalized by the number of trials) and the accuracy of model prediction for the rat's choices (percentage correct) were reduced following the lesions (**Fig. 6n**,**o**). No significant changes in any of these parameters were observed after sham lesions except for a reduced proportion of lose-stay trials (**Fig. 6b–o**).

DISCUSSION

We examined neuronal activity related to choice and value in two regions of the rodent motor cortex. Neural signals for the rat's upcoming goal choice arose in the rostral AGm several hundred milliseconds before behavioral manifestation of the rat's goal choice. The AGm also conveyed significant decision value and chosen value signals before and after a choice was made, respectively. By contrast, these neural signals arose later and less frequently in the AGl. Behaviorally, selective AGm lesions altered a rat's choice behavior so that it was less dependent on values estimated from the rat's experience. Taken together, these results suggest that the AGm, but not the AGl, is involved in both the valuation and selection of a rat's voluntary actions.

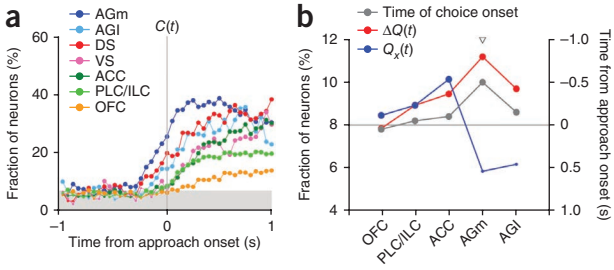

Figure 7 Regional variations in neural signals related to valuation and choice in rodent frontal cortex and striatum. (**a**) Time courses of neural signals for upcoming action selection. (**b**) Fractions of neurons encoding at least one action value ($Q_x(t)$; blue, corrected for multiple comparisons) or decision value ($\Delta Q(t)$, red) during the last 1 s of the delay stage (left axis). The onset time of the upcoming choice signal is also indicated for each region in gray (right axis). Large dots denote significant fractions; small dots, insignificant fractions (binomial test, $\alpha = 0.05$). The triangle indicates a significant difference between the fraction of action value– and decision value–encoding neurons (χ^2-test, $P < 0.05$). PLC/ILC, prelimbic and infralimbic cortex; DS, dorsal striatum; VS, ventral striatum.

Future-choice signals in the rat brain

Our previous investigations using free-choice tasks did not find clear preparatory signals related to action selection in the medial PFC (ACC, prelimbic cortex and infralimbic cortex), lateral OFC, dorsal striatum or ventral striatum in rats[2,8] (**Fig. 7a**). Choice behavior of the rats in these studies was well accounted for by reinforcement learning models, suggesting that the failure to find clear choice signals was not caused by the rats making random and impulsive choices. Although a previous study demonstrated upcoming action selection signals in the superior colliculus of rats, the task used in that study was not a free-choice task but an odor discrimination task, and the earliest onset of choice-related activity was only ~300 ms before movement initiation[20]. Thus, upcoming choice signals found in the rostral AGm seem to be the earliest unambiguous action selection signals discovered so far in the rat brain under a free-choice condition. It is notable that the rostral AGm sends direct projections to the superior colliculus[21], raising the possibility that action selection signals observed in the superior colliculus might originate in the AGm. Disruptive effects of AGm lesions on the rats' choice behavior also support this possibility. Because our results were obtained from freely moving animals, we cannot completely rule out the possibility that the advanced action selection signals in the AGm were due to subtle, undetected variations in the rat's behavior. Nevertheless, the physiological and behavioral results obtained in the present study provide converging evidence for a primary role of the rostral AGm in action selection during a dynamic foraging task.

AGm and supplementary motor area

The AGl is regarded as a major part of the primary motor cortex because it receives strong projections from the ventrolateral, but not mediodorsal, nucleus of the thalamus[22], sends direct projections to the spinal cord[23,24] and evokes movements when stimulated with low intensity electrical pulses[23,25,26]. By contrast, the AGm has been proposed to be homologous to the premotor cortex (PMC) and supplementary motor area (SMA) as well as frontal and supplementary eye fields in primates[21,23,25–29]. The rostral part of the AGm, in particular, has frequently been proposed to be homologous to the SMA in primates[23,25–27] because it receives inputs from both the ventrolateral nucleus and mediodorsal nucleus of the thalamus[22,30], sends strong projections to the primary motor cortex (that is, AGl)[21,22], contains

a second motor representation of the body[26,31] and, although it sends direct projections to the spinal cord[24], does not readily evoke movements when stimulated electrically[23,25,26]. All of these are characteristics of the SMA in primates[32]. Thus, although the homology between rat and primate motor cortical areas is not entirely clear[33], the rodent rostral AGm and primate SMA seem to share multiple anatomical and functional characteristics.

It is notable that substantial evidence highlights a critical role for the primate SMA in action selection under free-choice conditions[32,34]. SMA lesions often cause an inability to generate spontaneous movements of the contralateral limb, and sometimes cause the alien-limb syndrome in which the contralateral arm produces unwanted spontaneous movements, such as grasping nearby objects. Physiological studies have shown discharges of SMA neurons and readiness potentials over the SMA before movement onset, and brain imaging studies have found activity in the SMA and pre-SMA during a free-choice task[32]. Similarly, neural signals for upcoming saccades during a free-choice task arose earlier in the SEF than in the frontal eye field and lateral intraparietal cortex[14]. Collectively, these and our results suggest that the supplementary motor regions (SMA, pre-SMA and SEF) in monkeys and the rostral AGm in rats might be part of the neural system where the future action is selected and propagated to downstream motor structures, such as the primary motor cortex and superior colliculus, for execution under free-choice conditions. Considering that different neural systems might be in charge of final action selection under different behavioral conditions[34,35], it will be important for future studies to compare relative time courses of neural signals for upcoming action across different parts of the rodent brain during different behavioral tasks.

Convergence of choice and value signals in the AGm

Our results indicate the involvement of the rostral AGm not only in action selection but also in valuation, which is consistent with the finding that AGm activity is modulated by expected reward[36]. The SMA and PMC in monkeys also convey signals related to upcoming choice[32,37] as well as to expected reward[38–40]. Similarly, neurons in the primate superior colliculus convey both choice- and value-related signals[41]. Thus, coexistence of choice and value signals in motor structures might be a common feature across different species. However, the findings that expected outcome-dependent signals were stronger in the posterior parts of the lateral frontal cortex[38] and similarly modulated by expected reward and penalty, unlike in the OFC[39], led to the suggestion that such signals might reflect motivation-regulated motor preparation rather than subjective values of specific actions. In our task, the level of motivation before the rat's choice is presumably similar across trials, because the sum of reward probabilities was held constant. Therefore, it is difficult to explain decision value signals, which were found well before upcoming choice signals, in terms of motivation-related movement preparation. Further analyses also showed that chosen value signals are unlikely to represent motivation-dependent motor preparation (**Supplementary Fig. 6**). These results suggest that the value-related neural signals observed in the rostral AGm indeed represent values rather than movement preparation signals that are modulated by motivation.

Role of AGm in value-based action selection

The results obtained from the lesion experiments are also consistent with neurophysiological findings. The rats showed no obvious motor deficits following AGm lesions, indicating that the AGm is not involved in direct control of motor output. However, the lesioned rats were less likely to switch their choices after failing to obtain a reward (lose–switch) and to choose the goal with a higher reward probability, suggesting a deficit in the process of modifying future choices adaptively according to previous choice outcomes. When a reinforcement learning model was applied to the choice data, learning rate did not change with AGm lesions, suggesting that the rat's ability to update values was not completely lost, which is consistent with widespread value signals found in multiple areas of the rat brain[2,8]. On the other hand, the lesioned rats showed increased randomness in action selection (that is, low inverse temperature), indicating that their action selection became less dependent on values. Similarly, the AGm-lesioned rats tended to repeat a goal choice that was associated with a lower action value than the alternative, indicating that AGm-lesioned rats failed to adjust action selection according to altered action values.

Interestingly, the effect of AGm lesions on lose-switch was temporary, whereas the effects of lesions on other parameters lasted for the entire post-lesion sessions, suggesting that action selection functions of the AGm might be partially taken over by other brain structures. Perhaps relatively simple choice behavior such as lose-switch can be resumed by other brain structures such as the basal ganglia[42], whereas more elaborate value-based action selection requires the AGm. Collectively, our results suggest that the AGm is crucial in flexible action selection based on internally represented values.

Relationship with other brain structures

The valuation process in the AGm might not be independent of other brain structures. In rats, lesions to either the OFC or dorsal striatum impair reversal learning, and lesions to the OFC also impair reinforcer devaluation[43,44]. Thus, the AGm is unlikely to operate as a stand-alone module to serve valuation and choice functions. We found that the strength of decision value signals increases as one moves from the OFC to medial PFC and AGm, whereas the opposite pattern was observed for the strength of action value signals (**Fig. 7b**). This raises the possibility that absolute value signals are transformed into relative value signals in the structures of the rat brain that are involved in action selection, which might also be the case in monkeys[45]. The AGm might require afferent action value signals from such brain structures as the OFC and dorsal striatum in order to compute decision value signals.

METHODS

Methods and any associated references are available in the online version of the paper at http://www.nature.com/natureneuroscience/.

Note: Supplementary information is available on the Nature Neuroscience website.

ACKNOWLEDGMENTS

We thank C. Lee for discussion, P. Nachev for commenting on the manuscript, J.W. Ghim for helping with analysis and E. Seuter for proofreading the manuscript. This work was supported by a grant from the Brain Research Center of the 21st Century Frontier Research Program, a Korea National Research Foundation grant (2011-0015618), the Cognitive Neuroscience Program, and the Original Technology Research Program for Brain Science (2011-0019209) funded by the Ministry of Education, Science and Technology, Korea (to M.W.J.), and the US National Institutes of Health (to D.L.).

AUTHOR CONTRIBUTIONS

J.H.S. was involved in all aspects of the study. S.J. performed the lesion experiments. M.W.J. and D.L. contributed to the design of the experiments, data analysis and manuscript preparation.

COMPETING FINANCIAL INTERESTS

The authors declare no competing financial interests.

Published online at http://www.nature.com/natureneuroscience.
Reprints and permissions information is available online at http://www.nature.com/reprints/index.html.

1. Samejima, K., Ueda, Y., Doya, K. & Kimura, M. Representation of action-specific reward values in the striatum. *Science* **310**, 1337–1340 (2005).
2. Kim, H., Sul, J.H., Huh, N., Lee, D. & Jung, M.W. Role of striatum in updating values of chosen actions. *J. Neurosci.* **29**, 14701–14712 (2009).
3. Lau, B. & Glimcher, P.W. Value representations in the primate striatum during matching behavior. *Neuron* **58**, 451–463 (2008).
4. Platt, M.L. & Glimcher, P.W. Neural correlates of decision variables in parietal cortex. *Nature* **400**, 233–238 (1999).
5. Sugrue, L.P., Corrado, G.S. & Newsome, W.T. Matching behavior and the representation of value in the parietal cortex. *Science* **304**, 1782–1787 (2004).
6. Seo, H., Barraclough, D.J. & Lee, D. Lateral intraparietal cortex and reinforcement learning during a mixed-strategy game. *J. Neurosci.* **29**, 7278–7289 (2009).
7. Seo, H. & Lee, D. Temporal filtering of reward signals in the dorsal anterior cingulate cortex during a mixed-strategy game. *J. Neurosci.* **27**, 8366–8377 (2007).
8. Sul, J.H., Kim, H., Huh, N., Lee, D. & Jung, M.W. Distinct roles of rodent orbitofrontal and medial prefrontal cortex in decision making. *Neuron* **66**, 449–460 (2010).
9. Padoa-Schioppa, C. & Assad, J.A. Neurons in the orbitofrontal cortex encode economic value. *Nature* **441**, 223–226 (2006).
10. Roesch, M.R., Taylor, A.R. & Schoenbaum, G. Encoding of time-discounted rewards in orbitofrontal cortex is independent of value representation. *Neuron* **51**, 509–520 (2006).
11. Seo, H. & Lee, D. Behavioral and neural changes after gains and losses of conditioned reinforcers. *J. Neurosci.* **29**, 3627–3641 (2009).
12. Schultz, W. Predictive reward signal of dopamine neurons. *J. Neurophysiol.* **80**, 1–27 (1998).
13. Barraclough, D.J., Conroy, M.L. & Lee, D. Prefrontal cortex and decision making in a mixed-strategy game. *Nat. Neurosci.* **7**, 404–410 (2004).
14. Coe, B., Tomihara, K., Matsuzawa, M. & Hikosaka, O. Visual and anticipatory bias in three cortical eye fields of the monkey during an adaptive decision-making task. *J. Neurosci.* **22**, 5081–5090 (2002).
15. Pesaran, B., Nelson, M.J. & Andersen, R.A. Free choice activates a decision circuit between frontal and parietal cortex. *Nature* **453**, 406–409 (2008).
16. Louie, K. & Glimcher, P.W. Separating value from choice: delay discounting activity in the lateral intraparietal area. *J. Neurosci.* **30**, 5498–5507 (2010).
17. Kennerley, S.W., Dahmubed, A.F., Lara, A.H. & Wallis, J.D. Neurons in the frontal lobe encode the value of multiple decision variables. *J. Cogn. Neurosci.* **21**, 1162–1178 (2009).
18. Kim, Y.B. *et al.* Encoding of action history in the rat ventral striatum. *J. Neurophysiol.* **98**, 3548–3556 (2007).
19. Huh, N., Jo, S., Kim, H., Sul, J.H. & Jung, M.W. Model-based reinforcement learning under concurrent schedules of reinforcement in rodents. *Learn. Mem.* **16**, 315–323 (2009).
20. Felsen, G. & Mainen, Z.F. Neural substrates of sensory-guided locomotor decisions in the rat superior colliculus. *Neuron* **60**, 137–148 (2008).
21. Reep, R.L., Corwin, J.V., Hashimoto, A. & Watson, R.T. Efferent connections of the rostral portion of medial agranular cortex in rats. *Brain Res. Bull.* **19**, 203–221 (1987).
22. Donoghue, J.P. & Parham, C. Afferent connections of the lateral agranular field of the rat motor cortex. *J. Comp. Neurol.* **217**, 390–404 (1983).
23. Donoghue, J.P. & Wise, S.P. The motor cortex of the rat: cytoarchitecture and microstimulation mapping. *J. Comp. Neurol.* **212**, 76–88 (1982).
24. Miller, M.W. The origin of corticospinal projection neurons in rat. *Exp. Brain Res.* **67**, 339–351 (1987).
25. Sanderson, K.J., Welker, W. & Shambes, G.M. Reevaluation of motor cortex and of sensorimotor overlap in cerebral cortex of albino rats. *Brain Res.* **292**, 251–260 (1984).
26. Neafsey, E.J. *et al.* The organization of the rat motor cortex: a microstimulation mapping study. *Brain Res.* **396**, 77–96 (1986).
27. Reep, R.L., Goodwin, G.S. & Corwin, J.V. Topographic organization in the corticocortical connections of medial agranular cortex in rats. *J. Comp. Neurol.* **294**, 262–280 (1990).
28. Passingham, R.E., Myers, C., Rawlins, N., Lightfoot, V. & Fearn, S. Premotor cortex in the rat. *Behav. Neurosci.* **102**, 101–109 (1988).
29. Akintunde, A. & Buxton, D.F. Differential sites of origin and collateralization of corticospinal neurons in the rat: a multiple fluorescent retrograde tracer study. *Brain Res.* **575**, 86–92 (1992).
30. Reep, R.L., Corwin, J.V., Hashimoto, A. & Watson, R.T. Afferent connections of medial precentral cortex in the rat. *Neurosci. Lett.* **44**, 247–252 (1984).
31. Wang, Y. & Kurata, K. Quantitative analyses of thalamic and cortical origins of neurons projecting to the rostral and caudal forelimb motor areas in the cerebral cortex of rats. *Brain Res.* **781**, 135–147 (1998).
32. Nachev, P., Kennard, C. & Husain, M. Functional role of the supplementary and pre-supplementary motor areas. *Nat. Rev. Neurosci.* **9**, 856–869 (2008).
33. Uylings, H.B. & van Eden, C.G. Qualitative and quantitative comparison of the prefrontal cortex in rat and in primates, including humans. *Prog. Brain Res.* **85**, 31–62 (1990).
34. Tanji, J. The supplementary motor area in the cerebral cortex. *Neurosci. Res.* **19**, 251–268 (1994).
35. Buschman, T.J. & Miller, E.K. Top-down versus bottom-up control of attention in the prefrontal and posterior parietal cortices. *Science* **315**, 1860–1862 (2007).
36. Kargo, W.J., Szatmary, B. & Nitz, D.A. Adaptation of prefrontal cortical firing patterns and their fidelity to changes in action-reward contingencies. *J. Neurosci.* **27**, 3548–3559 (2007).
37. Hoshi, E. & Tanji, J. Distinctions between dorsal and ventral premotor areas: anatomical connectivity and functional properties. *Curr. Opin. Neurobiol.* **17**, 234–242 (2007).
38. Roesch, M.R. & Olson, C.R. Impact of expected reward on neuronal activity in prefrontal cortex, frontal and supplementary eye fields and premotor cortex. *J. Neurophysiol.* **90**, 1766–1789 (2003).
39. Roesch, M.R. & Olson, C.R. Neuronal activity related to reward value and motivation in primate frontal cortex. *Science* **304**, 307–310 (2004).
40. Sohn, J.W. & Lee, D. Order-dependent modulation of directional signals in the supplementary and presupplementary motor areas. *J. Neurosci.* **27**, 13655–13666 (2007).
41. Thevarajah, D., Mikulic, A. & Dorris, M.C. Role of the superior colliculus in choosing mixed-strategy saccades. *J. Neurosci.* **29**, 1998–2008 (2009).
42. Balleine, B.W., Delgado, M.R. & Hikosaka, O. The role of the dorsal striatum in reward and decision-making. *J. Neurosci.* **27**, 8161–8165 (2007).
43. Schoenbaum, G., Roesch, M.R. & Stalnaker, T.A. Orbitofrontal cortex, decision-making and drug addiction. *Trends Neurosci.* **29**, 116–124 (2006).
44. Ragozzino, M.E. The contribution of the medial prefrontal cortex, orbitofrontal cortex, and dorsomedial striatum to behavioral flexibility. *Ann. NY Acad. Sci.* **1121**, 355–375 (2007).
45. Kable, J.W. & Glimcher, P.W. The neurobiology of decision: consensus and controversy. *Neuron* **63**, 733–745 (2009).
46. Paxinos, G. & Watson, C. *The Rat Brain in Stereotaxic Coordinates* (Academic Press, San Diego, 1998).

ONLINE METHODS

Behavioral task. Rats were trained in a free binary choice task on a modified figure 8–shaped maze (**Fig. 1a**) as in our previous studies[2,8,19]. The rat had to navigate from the central stem to one of the two goal sites to obtain water reward (30 μl) in each trial. The reward was controlled by a concurrent variable ratio–variable ratio reinforcement schedule, in which each choice contributed to the ratio requirement of both goals[19]. Thus, in each trial, reward could be available at neither, either or both goals. If a particular goal was baited with a reward, it remained available, although it did not accumulate, in the subsequent trials until the rat visited that goal (referred to as a 'dual assignment with hold' task)[47,48]. The rats performed four blocks of trials in each recording session. The number of trials in each block was 35 plus a random number drawn from a geometric mean of 5 and truncated at 45. Reward probability of a goal was constant within a block of trials but was changed across blocks without any sensory cues. The rats therefore had to detect changes in relative reward probabilities by trial and error. The following four combinations of reward probabilities were used in each session: 0.72:0.12, 0.63:0.21, 0.21:0.63 and 0.12:0.72. The sequence of reward probabilities was determined randomly with the constraint that the option with the higher reward probability always changed its location at the beginning of a new block. The rat's head position was monitored by tracking an array of light-emitting diodes mounted on the headstage at 60 Hz. The experimental protocol was approved by the Institutional Animal Care and Use Committee of the Ajou University School of Medicine.

Behavioral stages. Each trial consisted of the delay, go, approach to reward, reward consumption and return stages (**Fig. 1a**), as in our previous studies[2,8]. A trial began when the rat returned from a goal site to the central stem through the lateral alley and broke the central photobeam (**Fig. 1a**). A 2-s delay was imposed at the outset of each trial by raising the central connecting bridge (delay stage). The bridge was lowered at the end of the delay stage, allowing the rat to move forward (go stage). The approach stage was the time period during which the animal turned and ran toward either the goal site on the upper alley. The onset of the approach stage was determined separately for each behavioral session as the time when the left–right positions became significantly different for the left-choice and right-choice trials (*t*-test, $P < 0.05$) for the first time near the upper branching point (**Supplementary Fig. 1**)[2,8]. Thus, the onset of the approach stage marked the first behavioral manifestation of the rat's goal choice at the branching point. The reward stage began when the rat broke a photobeam that was placed 6 cm in front of the water delivery nozzle, which triggered an immediate delivery of water in rewarded trials. The return stage began when the rat broke a photobeam that was placed 11 cm away from the water delivery nozzle and ended when the animal returned to the central stem and broke the central photobeam (that is, the beginning of the next trial). The mean durations of the five behavioral stages were (mean ± s.d.) 2.00 ± 0.00 s (delay), 0.70 ± 0.18 s (go), 0.83 ± 0.22 s (approach), 6.13 ± 1.50 s (reward), and 1.97 ± 0.23 s (return stage). The mean durations of the reward stage for the rewarded and unrewarded trials were 8.56 ± 1.95 s and 2.23 ± 0.89 s, respectively. Thus, the rats stayed longer in the reward area in rewarded than unrewarded trials, although they licked the water delivery nozzle in most unrewarded trials, as in rewarded trials. Therefore, we cannot exclude the possibility that movement-dependent neuronal activity might have contributed to reward-related neuronal activity during the reward stage.

Logistic regression analysis. Effects of previous choices and their outcomes on the rat's goal choice were estimated using the following logistic regression model[2,48]:

$$\log\left(\frac{p_L(i)}{p_R(i)}\right) = \sum_{j=1}^{10} \gamma_j^R (R_L(i-j) - R_R(i-j)) + \sum_{j=1}^{10} \gamma_j^C (C_L(i-j) - C_R(i-j)) + \gamma_0$$

where $p_L(i)$ (or $p_R(i)$) is the probability of selecting the left (or right) goal in the ith trial. The variables $R_L(i)$ (or $R_R(i)$) and $C_L(i)$(or $C_R(i)$) are reward delivery at the left (or right) goal (0 or 1) and the left (or right) goal choice (0 or 1) in the ith trial, respectively. The coefficients γ_j^R and γ_j^C denote the effect of past rewards and choices, respectively, and γ_0 is a bias term. The numbers of total trials used in the regression for the three rats were 2,070, 1,907 and 2,112.

Reinforcement learning model. Our previous study[19] showed that the animal's choice behavior in the current task is better explained by a model-based than a model-free reinforcement learning algorithm. We therefore used a model-based reinforcement learning algorithm that takes into consideration that the reward probability of the unchosen target increases as a function of the number of consecutive alternative choices[19] ('stacked probability' algorithm; see **Supplementary Note**). The stacked probability algorithm was indeed superior in explaining a rat's choice behavior to a model-free reinforcement learning algorithm that changed only the values of chosen (but not unchosen) actions (**Supplementary Table 2**). However, results from the analyses of neural data were similar regardless of which reinforcement learning algorithm was used (**Supplementary Fig. 7**). Parameters α (learning rate) and β (inverse temperature) were estimated for the entire data set from each rat using a maximum likelihood procedure[2,8]. The values of α and β for three rats were 0.58 and 2.02, 0.55 and 2.04, and 0.32 and 2.59, respectively. To compare the rat's performance to an optimal learner, we determined the optimal values for the parameters α and β of the stacked probability algorithm by selecting the combination that yielded the maximal amount of rewards (average of 10 simulations) among 400 pairs of α (0.05 to 1.0 in steps of 0.05) and β (0.25 to 5.0 in steps of 0.25) values.

Unit recording. Two sets of six tetrodes were implanted in the right AGm (2.7–3.2 mm anterior and 1.0 mm lateral to the bregma) and right AGl (2.7–3.2 mm anterior and 2.7 mm lateral to the bregma; **Fig. 2**) of three well trained rats under deep sodium pentobarbital anesthesia (50 mg per kilogram body weight). After at least 1 week of surgery recovery time, tetrodes were gradually lowered to obtain isolated action potentials from single neurons. Once the recording began, tetrodes were advanced for a maximum of 75 μm per day. Unit signals were amplified ×10,000, filtered between 0.6 and 6 KHz, digitized at 32 KHz and stored on a personal computer using a Cheetah data acquisition system. Unit signals were also recorded with the rats placed on a pedestal before and after each experimental session to examine the stability of recorded unit signals. When recordings were completed, small marking lesions were made by passing an electrolytic current (50 μA, 30 s, cathodal) through one channel of each tetrode and recording locations were verified histologically[49].

Isolation and classification of units. Single units were isolated by manually clustering spike waveform parameters (MClust 3.4, http://redishlab.neuroscience.umn.edu/MClust/MClust.html; **Supplementary Fig. 8a**). Recorded units were classified into two categories of broad-spiking neurons (putative pyramidal cells) and narrow-spiking neurons (putative interneurons; **Supplementary Fig. 8b**). The majority of the analyzed units were broad-spiking neurons (AGm: $n = 350$, 85.2%; AGl: $n = 175$, 77.1%). Although both types of neurons were included in the analyses, essentially the same results were obtained when narrow-spiking neurons were excluded from the analyses (data not shown).

Multiple regression analysis. Modulation of neuronal activity according to the rat's choice or its outcome was analyzed using the following regression model:

$$S(t) = a_0 + a_1C(t) + a_2C(t-1) + a_3C(t-2) + a_4R(t) + a_5R(t-1) + a_6R(t-2) + a_7X(t) + a_8X(t-1) + a_9X(t-2) + \varepsilon(t) \quad (1)$$

where $S(t)$ indicates spike discharge rate, $C(t)$, $R(t)$ and $X(t)$ represent the rat's choice (left or right; dummy variable, −1 or 1), its outcome (reward or no reward; dummy variable, −1 or 1) and their interaction (dummy variable, −1 or 1), respectively, in trial t. $\varepsilon(t)$ is the error term and a_0 through a_9 are the regression coefficients.

Neuronal activity related to values was examined using the following regression model, as in our previous study[8]:

$$S(t) = a_0 + a_1C(t) + a_2R(t) + a_3X(t) + a_4\Delta Q(t) + a_5Q_c(t) + a_6C(t-1) + a_7R(t-1) + A(t) + \varepsilon(t) \quad (2)$$

where $\Delta Q(t)$ and $Q_c(t)$ denote decision value and chosen value, which were estimated using the stacked-probability model-based reinforcement learning algorithm (or Rescorla–Wagner rule for the analyses shown in **Supplementary Fig. 7**), respectively. A slow drift in the firing rates can potentially inflate the estimate of value-related signals[8]. To control for this, the above model included

a set of autoregressive terms, indicated by $A(t)$, that consisted of spike discharge rates during the same epoch in the previous three trials as the following:

$$A(t) = a_{10}S(t-1) + a_{11}S(t-2) + a_{12}S(t-3)$$

where a_{10} through a_{12} are regression coefficients.

Population decoding of goal choice. We examined how well the activity of a simultaneously recorded neuronal ensemble predicted rat's goal choice using a template matching procedure with leave-one-out cross validation[50] (**Fig. 3c**). The analysis was applied to the activity of neuronal ensembles containing ≥5 simultaneously recorded neurons after matching the distributions of neuronal ensemble size for the two regions by randomly dropping neurons from oversized AGm ensembles (size of analyzed ensembles, 5–21 neurons; 10.1 ± 5.0, mean ± s.d.). We then calculated the percentage of trials for which neuronal ensemble activity during a 100-ms sliding time window (50-ms time steps) correctly predicted the rat's goal choice (percentage correct decoding).

Determination of choice signal onset. The latency of upcoming choice signals was determined for the entire neural population as well as for individual neurons. For the neural population, we examined the fraction of neurons encoding the current choice signal using a multiple regression analysis (equation (1)) at a fine temporal resolution (a moving window of 100 ms that was advanced in 50-ms time steps; **Fig. 3b**). The onset of the upcoming choice signal was determined as the first time point at which the fraction of upcoming choice-encoding neurons exceeded and remained significantly higher than chance level (binomial test, $\alpha = 0.05$) for a minimum of 250 ms (5 bins) within 1-s time periods before and after the approach onset[8]. For individual neurons, we examined whether neuronal activity that was associated with the left versus right choice trials during a 100-ms sliding time window (with 50-ms time steps) was significantly different based on a t-test ($\alpha = 0.05$). The onset of the upcoming choice signal was determined as the first time point at which the left versus right choice-associated neuronal activity was significantly different for a minimum of 150 ms (3 bins) within 1-s time periods before and after the approach onset (**Fig. 3e**).

Test of AGm lesion effects. Twelve more rats were trained in the same task for 20 d, as described in our previous study[19]. After testing the rats for another 10 d to establish pre-lesion baseline performance (148–178 trials per session), 0.1 M quinolinic acid (lesion group, $n = 6$ rats) or 0.9% saline (vehicle; sham lesion group, $n = 6$ rats) was infused into five locations of the rostral AGm (2.7 mm anterior and 1 mm lateral to bregma, 0.2 µl; 3.2 mm anterior and 1 mm lateral, 0.2 µl; 3.7 mm anterior and1.2 mm lateral, 0.2 µl; 4.2 mm anterior and 1 mm lateral, 0.15 µl; 4.2 mm anterior and 3 mm lateral, 0.15 µl) in each hemisphere under deep sodium pentobarbital anesthesia (50 mg per kg). After 1 week of recovery from surgery, the rats were tested again in the same task (148–173 trials per session) for 10 d. The rats were then overdosed with sodium pentobarbital and their brains were processed according to a standard histological procedure, as previously described[49]. The extents of lesions were determined based on light microscopic examinations of histological sections (40 µm thick) that were stained with cresyl violet. One rat was discarded from the lesion group because of incomplete lesions (a very small lesion was detected on only one side of the brain) and one sham-lesioned rat died during surgery, leaving five rats for each group.

Statistical analysis. Statistical significance of a regression coefficient was determined using a t-test, and statistical significance of the fraction of neurons for a given variable with a binomial test. Effects of AGm lesions on behavioral parameters were tested with two-way repeated measure analysis of variance followed by paired t-tests. $P < 0.05$ was used as the criterion for a significant statistical difference unless noted otherwise. Data are expressed as mean ± s.e.m. unless noted otherwise.

47. Staddon, J.E., Hinson, J.M. & Kram, R. Optimal choice. *J. Exp. Anal. Behav.* **35**, 397–412 (1981).
48. Lau, B. & Glimcher, P.W. Dynamic response-by-response models of matching behavior in rhesus monkeys. *J. Exp. Anal. Behav.* **84**, 555–579 (2005).
49. Baeg, E.H. *et al.* Fast spiking and regular spiking neural correlates of fear conditioning in the medial prefrontal cortex of the rat. *Cereb. Cortex* **11**, 441–451 (2001).
50. Baeg, E.H. *et al.* Dynamics of population code for working memory in the prefrontal cortex. *Neuron* **40**, 177–188 (2003).

doi:10.1038/nn.2881

Corrigendum: Role of rodent secondary motor cortex in value-based action selection

Jung Hoon Sul, Suhyun Jo, Daeyeol Lee & Min Whan Jung

Nat. Neurosci. **14, 1202–1208 (2011); published online 14 August 2011; corrected after print 12 April 2012**

In the version of this article initially published, the percentages of neurons encoding action value $Q_x(t)$ shown in Figure 7b were incorrect owing to a mistake in the computer code used to analyze the data:

Initial version

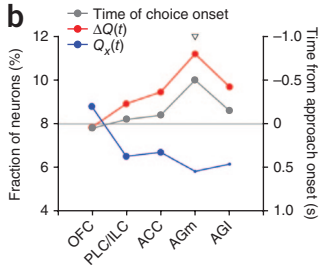

Corrected version

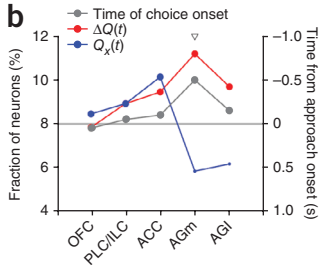

The error has been corrected in the HTML and PDF versions of the article.